Repurposing the FDA-Approved Antiviral Drug Ribavirin as Targeted Therapy for Nasopharyngeal Carcinoma

Sakibul Huq[1], Joshua Casaos[1], Riccardo Serra[1], Michael Peters[1], Yuanxuan Xia[1], Andy S. Ding[1], Jeff Ehresman[1], Jayanidhi N. Kedda[1], Manuel Morales[1], Noah L. Gorelick[1], Tianna Zhao[1], Wataru Ishida[1], Alexander Perdomo-Pantoja[1], Arba Cecia[1], Chenchen Ji[1], Ian Suk[2], David Sidransky[3], Mariana Brait[3], Henry Brem[1,4], Nicolas Skuli[1], and Betty Tyler[1]

ABSTRACT

Nasopharyngeal carcinoma (NPC) is a squamous cell carcinoma with a proclivity for systemic dissemination, leading many patients to present with advanced stage disease and fail available treatments. There is a notable lack of targeted therapies for NPC, despite working knowledge of multiple proteins with integral roles in NPC cancer biology. These proteins include EZH2, Snail, eIF4E, and IMPDH, which are all overexpressed in NPC and correlated with poor prognosis. These proteins are known to be modulated by ribavirin, an FDA-approved hepatitis C antiviral that has recently been repurposed as a promising therapeutic in several solid and hematologic malignancies. Here, we investigated the potential of ribavirin as a targeted anticancer agent in five human NPC cell lines. Using cellular growth assays, flow cytometry, BrdU cell proliferation assays, scratch wound assays, and invasion assays, we show *in vitro* that ribavirin decreases NPC cellular proliferation, migration, and invasion and promotes cell-cycle arrest and cell death. Modulation of EZH2, Snail, eIF4E, IMPDH, mTOR, and cyclin D1 were observed in Western blots and enzymatic activity assays in response to ribavirin treatment. As monotherapy, ribavirin reduced flank tumor growth in multiple NPC xenograft models *in vivo*. Most importantly, we demonstrate that ribavirin enhanced the effects of radiotherapy, a central component of NPC treatment, both *in vitro* and *in vivo*. Our work suggests that NPC responds to ribavirin-mediated EZH2, Snail, eIF4E, IMPDH, and mTOR changes and positions ribavirin for clinical evaluation as a potential addition to our NPC treatment armamentarium.

Introduction

Nasopharyngeal carcinoma (NPC) is a malignant squamous cell carcinoma most frequently seen in the pharyngeal recess whose hallmark is strong association with the Epstein-Barr Virus (EBV; ref. 1). NPC is endemic to southern China and has elevated incidence worldwide in northern Africa, the Inuits of Alaska, and Chinese immigrants in North America and Asia (2, 3). The standard of care for NPC is radiotherapy for local disease and combination chemoradiotherapy for advanced or metastatic disease (1, 4). Key therapies include antimetabolite and platinum-based therapies such as gemcitabine, cisplatin, and fluorouracil (1, 4, 5). These approaches can achieve favorable local control for early-stage disease; however, NPC has a propensity for systemic dissemination, leading many patients to fail treatment (5, 6). In addition, due to nonspecific presenting symptoms, nearly half of patients initially present with advanced stage, metastatic disease (1). There is consequently a significant clinical need for recurrent and late-stage NPC, which both carry dismal prognoses (7).

There is a notable lack of targeted therapies for NPC, despite working knowledge of multiple proteins with central roles in NPC cancer biology and significant prognostic value. These include Enhancer of Zeste Homolog 2 (EZH2), Snail, Eukaryotic Initiation Factor 4E (eIF4E), and Inosine Monophosphate Dehydrogenase (IMPDH). EZH2, a histone methyltransferase, is the catalytic subunit of polycomb repressive complex 2 and is considered to be a master regulator of transcription in both native and cancer biology (8). EZH2 protein is overexpressed in NPC, contributing to several oncogenic processes and poor prognosis (9–11). A known binding partner of EZH2, Snail, is also overexpressed in multiple cancers and may confer stem-like properties that induce epithelial-to-mesenchymal transitions (12, 13). In NPC, Snail and EZH2 form a complex to suppress E-cadherin and promote invasion and metastasis (10). Elevated nuclear expression of Snail protein is unsurprisingly associated with poor NPC prognosis (13). Another important feature of NPC is elevated protein expression of eIF4E, a critical effector of translation that has been associated with poor prognosis, drug resistance, and malignant transformation in approximately 30% of all cancers (14, 15). Finally, IMPDH is a biosynthetic enzyme involved in the conversion of inosine monophosphate to xanthosine monophosphate, the rate-limiting step in *de novo* synthesis of guanine nucleotides. Elevated IMPDH provides guanine nucleotides for rapidly dividing cells and has been implicated as a critical enzyme in cancer. Protein expression of the IMPDH isoform IMPDH2 has been associated with aggressive features and poor prognosis in NPC (16).

To date, EZH2, Snail, eIF4E, and IMPDH have not been clinically targeted in NPC, despite their known prognostic value. These proteins,

[1]Hunterian Neurosurgical Research Laboratory, Department of Neurosurgery, Johns Hopkins University School of Medicine, Baltimore, Maryland. [2]Department of Neurosurgery, Johns Hopkins University School of Medicine, Baltimore, Maryland. [3]Head and Neck Cancer Research Laboratory, Department of Otolaryngology and Head & Neck Surgery, Johns Hopkins University School of Medicine, Baltimore, Maryland. [4]Departments of Biomedical Engineering, Oncology, and Ophthalmology, Johns Hopkins University School of Medicine, Baltimore, Maryland.

Note: Supplementary data for this article are available at Molecular Cancer Therapeutics Online (http://mct.aacrjournals.org/).

S. Huq and J. Casaos are co-first authors. N. Skuli and B. Tyler are co-senior authors.

Corresponding Author: Betty Tyler, Johns Hopkins University, 1550 Orleans Street, CRB2 2M45, Baltimore, MD 21231. Phone: 410-502-8197; Fax: 410-614-0478; E-mail: btyler@jhmi.edu

Mol Cancer Ther 2020;19:1797–808

doi: 10.1158/1535-7163.MCT-19-0572

however, have all been reported to be modulated by ribavirin (structural name: 1-β-D-Ribofuranosyl-1,2,4-triazole-3-carboxamide; formula: C_8-H_{12}-N_4-O_5; ref. 17), a hepatitis C antiviral approved by the Food and Drug Administration (FDA) which has recently been found to have promising activity across cancers including leukemia, hepatocellular carcinoma, breast cancer, thyroid cancer, glioblastoma, and atypical teratoid/rhabdoid tumor (15, 18–23).

On the basis of this evidence, we sought to evaluate the efficacy of ribavirin as a novel targeted therapeutic for NPC. We assessed the effects of ribavirin in five human NPC cell lines (C666-1, CNE-2, HNE-1, HONE-1, and SUNE-1) *in vitro* and two of these cell lines (C666-1 and CNE-2) *in vivo*. We demonstrate *in vitro* that ribavirin impairs cell growth, promotes cell-cycle arrest, induces cell death, and reduces cell migration and invasion. These effects appear to be mechanistically mediated by targeting EZH2, Snail, eIF4E, mTOR, cyclin D1, and IMPDH. *In vivo*, ribavirin reduced tumor burden in separate xenograft models. Finally, we show that ribavirin sensitizes NPC to radiation, a foundational element of current treatment regimens, both *in vitro* and *in vivo*. Our work offers an opportunity to augment our treatment arsenal for NPC, particularly for recurrent and late-stage disease, by modulating known prognostic proteins with an FDA-approved drug well positioned for clinical evaluation.

Materials and Methods

Cell lines and cell culture

Human NPC cell lines C666-1, CNE-2, HNE-1, HONE-1, and SUNE-1 were provided by the Head and Neck Cancer Research Laboratory and Ambinder Laboratory (Johns Hopkins University, Baltimore, MD). All cells were authenticated and tested for *Mycoplasma*. Cells were maintained in RPMI medium (Lonza) supplemented with 10% FBS (Lonza) at 37°C in 5% CO_2-humidified incubators. Cells were treated with desired concentrations of ribavirin (Sigma-Aldrich), guanosine (Sigma-Aldrich), or ultrapure water (Invitrogen) as vehicle.

Cell growth viability assay

NPC cells were treated as indicated with desired concentrations of ribavirin, guanosine, or ultrapure water as vehicle. A total of 2.5×10^4 cells were plated for CNE-2, HNE-1, HONE-1, and SUNE-1 cells, and 1.0×10^5 cells were plated for C666-1 cells. Cells were collected and counted using the Malassez slide (Invitrogen) as described previously (19).

Flow cytometry

Cells were seeded in 6-well plates and treated with ribavirin for 24, 48, 72, or 96 hours then collected, washed in PBS (Invitrogen), and prepared for flow cytometry according to manufacturer's instructions. Cells were labeled with FITC-anti-Ki67 antibody (Abcam) for cell-cycle analysis and the APC-AnnexinV/Dead Cell Apoptosis Kit (Invitrogen) for cell death. Cells were then analyzed on a flow cytometer (FACSCalibur, Becton Dickinson). Analyses were performed using FlowJo software (FlowJo LLC).

BrdU cell proliferation assay

A total of 1.0×10^3 cells were seeded in 96-well plates and treated with ribavirin for 48 hours and then prepared for the BrdU cell proliferation immunoassay (Millipore Sigma) according to the manufacturer's instructions. Results were quantified by spectrophotometry and normalized relative to controls.

Scratch wound/migration assay

Cells were seeded in 6-well plates and allowed to form a confluent monolayer. Cells were then treated as indicated, and a wound was made using a plastic pipette tip. Media and ribavirin or water were replaced, and cells were incubated for 12 hours to allow migration. Images were acquired from identical locations along each scratch using a Zeiss Observer Z.1 AX10 microscope (Zeiss), and cell migration was quantified at 0, 8, and 12 hours after scratch using ImageJ software. These early time points precluded confounding effects of reduced proliferation and cell death on migration.

Invasion assay

Invasion assays were performed in 24-well plates using Corning BioCoat Matrigel Invasion Chambers (Corning) with Matrigel-coated inserts. Cells (1.0×10^5) were pretreated with ribavirin or control and placed in the top chamber with serum-free medium. They invaded toward the bottom chamber, which contained culture medium with 10% FBS. After 24 hours, the bottom of each insert was fixed and stained with crystal violet. Invading cells were quantified using light microscopy.

NPC genomic dataset

A publicly available NPC genomic dataset (24) containing NPC and adjacent nasopharyngeal epithelium from 41 patients was analyzed through Oncomine (Thermo Fisher Scientic). Gene expression data was stratified by TNM staging and statistical analysis was performed comparing NPC and control tissue.

Western blot analysis

Cells treated with ribavirin or control were lysed using RIPA buffer, and Western blots were performed using the following antibodies: anti-EZH2 (1/500, #MA5-18108, Thermo Fisher Scientific), anti-Snail (1/1,000, #ab180714, Abcam), anti-phospho (S209) eIF4E (1/1,000, #9742, Cell Signaling Technology), anti-eIF4E (1/1,000, #9741, Cell Signaling Technology), anti-IMPDH2 (1/1,000, AV54366, Sigma-Aldrich), anti-mTOR (1/1,000, #2983, Cell Signaling Technology), anti-phospho (S2448)-mTOR (1/1,000, #5536, Cell Signaling Technology), anti-cyclin D1 (1/1,000, #2978T, Cell Signaling Technology), and IgG HRP-linked whole antobody (1/30,000, GENA934, GE-Healthcare). Data were normalized to respective loading controls using an anti-GAPDH antibody (1/1,000, 607902, BioLegend).

IMPDH activity assay

An IMPDH Enzyme Activity Assay Kit was purchased from Biomedical Research Service Center (E-119, BMR) and used to measure enzymatic activity in C666-1, CNE-2, and HNE-1 cells treated with ribavirin (50 μmol/L) or vehicle control (H_2O). Cells were lysed and incubated with IMPDH Substrate and Assay Solutions (BMR) in a 96-well plate for spectrophotometric measurements to calculate enzymatic activity according to the manufacturer-provided protocol.

Histone methyltransferase assay

The EpiQuik Histone Methyltransferase Activity/Inhibition Assay Kit (H3K27) was purchased from Epigentek (P-3005-48, Epigentek) and used to measure histone methyltransferase activity at Histone H3, Lysine 27 in C666-1 and CNE-2 cells in the presence of ribavirin. Nuclear extracts of C666-1 and CNE-2 cells were prepared using the EpiQuik Nuclear Extraction Kit (Epigentek) and subsequently incubated with ribavirin (10 μmol/L, 50 μmol/L, 100 μmol/L). Spectrophotometric measurements were taken indicating levels of methylated

H3K27, and percentage of enzyme inhibition by ribavirin was calculated according to level of H3K27 in the control assay.

Clonogenic cell survival assay

The clonogenic cell survival assay was performed as described previously (25). NPC cells were treated with ribavirin and/or radiation (CIXD irradiator, Xstrahl) at indicated doses. Cells were incubated for 10 days, fixed with paraformaldehyde and stained with crystal violet. Plating efficiency and surviving fraction were quantified as described previously (25).

In vivo flank tumor xenograft experiments

Athymic immunodeficient mice (NU/NU athymic; Charles River) were anesthetized with pharmaceutical-grade anesthesia and analgesia and subcutaneously implanted with 2×10^6 NPC cells in PBS and Matrigel (Corning) in the right flank. Animals received daily intraperitoneal injections (200 μL) of pharmaceutical-grade ribavirin (100 mg/kg/day) or water vehicle. In the combination therapy experiment with ribavirin + radiation (XRT), flank tumors were irradiated with 5 Gray (Gy) over three fractions per the indicated schedule. When flank tumors approached size limits permitted by protocol, animals were perfused with intracardiac PBS and paraformaldehyde. All procedures were performed in accordance with the guidelines set forth by the Johns Hopkins University Animal Care and Use Committee (IACUC).

H&E staining and IHC

Mice were treated as above and sacrificed when indicated by IACUC protocol. Flank tumors were resected, fixed in formalin, paraffin-embedded, and sectioned into 7-μm slices. Hematoxylin and eosin (H&E) staining was performed. For IHC stains, sections were deparaffinized and rehydrated in a series of xylene and ethanol baths. Antigen retrieval was performed in citrate buffer at 95°C for 30 minutes. Endogenous peroxidase activity was blocked with 3% H_2O_2. Sections were incubated with Avidin and Biotin blocking solutions (#004303, Invitrogen) and incubated overnight at 4°C with rabbit monoclonal anti-cleaved caspase-3 antibody (1/400, #229, Biocare Medical). Protein staining was detected using the MultiLink + HRP label system (QP900-9LE, Biogenex) and Two-Component DAB (HK542-XAKE, Biogenex). Sections were counterstained with hematoxylin and dehydrated in a series of ethanol and xylene baths. Six images per tumor section were taken using the Zeiss Observer Z.1 AX10 microscope, and quantification of positively stained cells was performed using ImageJ software.

Statistical analysis

Unpaired *t* tests were used to calculate final *P* values using GraphPad Prism 8.0 (GraphPad). Data represent at least three independent experiments. Significance is represented by "*" where *, $P < 0.05$, **, $P < 0.01$, ***, $P < 0.001$, and ****, $P < 0.0001$.

Results

Ribavirin decreases NPC cell growth through cell-cycle arrest and cell death

We tested the effects of ribavirin on viability and proliferative properties of NPC in five different cell lines, including C666-1, the only available cell line natively positive for EBV. We first treated these cells with 10 μmol/L, 20 μmol/L, 50 μmol/L, or 100 μmol/L ribavirin and measured cell growth by counting viable cells at days 2, 4, and 6. Ribavirin decreased cell growth at 10 μmol/L in all cell lines tested (**Fig. 1A** and **B**; Supplementary Fig. S1A and S1B; Supplementary Table S1).

We then assessed NPC cell-cycle changes following ribavirin treatment using flow cytometry with propidium iodide (PI) and Ki67 staining. Daily ribavirin (50 μmol/L) for 48 hours significantly decreased the number of Ki67-positive cells in C666-1 (Ctrl: 48.7% vs. Rib: 38.3%) and CNE-2 cells (Ctrl: 44.9% vs. Rib: 37.0%; **Fig. 2A**). These results suggest that the reduced proliferation seen in NPC cells may be partly mediated by cell-cycle arrest in G_0. We complemented these findings with a BrdU cell proliferation assay, which demonstrated that daily ribavirin (50 μmol/L) for 48 hours significantly decreased BrdU incorporation into C666-1 (31.3% reduction) and CNE-2 (15.9% reduction) cells (**Fig. 2B**).

Because cell-cycle arrest can lead to apoptosis and cell death, we next used flow cytometry with Annexin-V (AnnV) and PI staining to study the effects of ribavirin on NPC cell death following 24, 48, 72, and 96 hours of treatment. We separately quantified populations of $AnnV^+/PI^-$ and $AnnV^+/PI^+$ cells to distinguish cells undergoing early and late apoptosis, respectively. This analysis demonstrated that the timing of cell death induction occurred in a cell line-dependent manner. In C666-1 cells, a significantly increased population of $AnnV^+/PI^-$ cells was seen following 48 and 72 hours of ribavirin treatment (Ctrl: 1.53% vs. Rib48 h: 5.12% vs. Rib72 h: 6.02%), while an $AnnV^+/PI^+$ population was not seen until 96 hours (Ctrl: 2.18% vs. Rib96 h: 5.26%; **Fig. 2C**). We coupled these findings with immunoblotting for PARP in C666-1 cells, which demonstrated an increase in cleaved PARP, representing cells undergoing apoptosis, at all time points following 12 hours of ribavirin treatment (Supplementary Fig. S2). In the other four cell lines tested, distinct populations of $AnnV^+/PI^-$ and $AnnV^+/PI^+$ cells were seen following 48 and 72 hours of treatment (**Fig. 2C**; Supplementary Table S1). Altogether, these findings suggest that ribavirin inhibits NPC cell growth by promoting cell-cycle arrest and inducing cell death.

Ribavirin reduces NPC cell migratory and invasive capacity

We sought to determine ribavirin's effects on NPC migration through scratch wound assays of the CNE-2, HNE-1, HONE-1, and SUNE-1 cell lines. We were unable to perform this assay on C666-1, because this cell line is only semiadherent. In all cell lines tested, ribavirin (50 μmol/L) significantly decreased the ability of NPC cells to close the wound compared with control cells by $t = 8$ hours (**Fig. 3A**; Supplementary Fig. S3). Using invasion assays with Matrigel-coated inserts in CNE-2, HNE-1, and HONE-1 cells, we also demonstrated that ribavirin (50 μmol/L) significantly decreased the invasive properties of NPC cells (**Fig. 3B**). Ribavirin may therefore provide an effective means of reducing the migratory and invasive capacity of NPC.

Potential mechanisms of ribavirin action in NPC cells

We next investigated the potential mechanisms of action involved in response to ribavirin treatment in NPC cells (**Fig. 4A–E**; Supplementary Fig. S4). A publicly available NPC genomic dataset (24) revealed increased mRNA expression of *EZH2* (Ctrl: 1.1 vs. NPC: 2.6) and *eIF4E* (Ctrl: 2.1 vs. NPC: 2.7) in NPC relative to normal adjacent nasopharynx (**Fig. 4A**). *IMPDH2* mRNA expression was not different between the two groups (Ctrl: 4.1 vs. NPC: 4.1). However, there was stronger *IMPDH2* expression in tissues with higher lymph node involvement relative to less lymph node involvement (N2: 4.5 vs. N1: 4.0; **Fig. 4A**). Of note, *Snail* mRNA was not detected using this dataset, although the literature suggests that it is expressed in NPC and associated with aggressive features (10, 13).

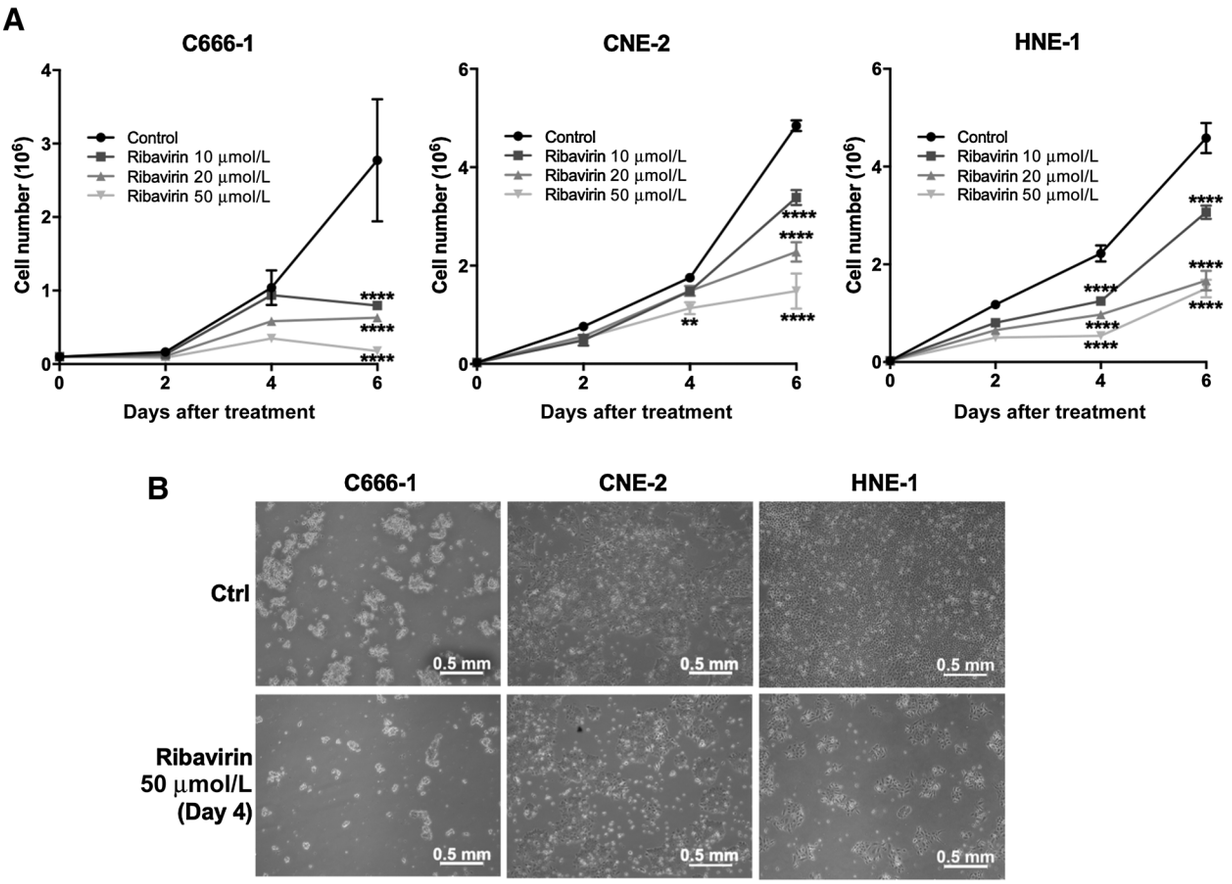

Figure 1.

Ribavirin inhibits NPC cell proliferation. **A,** Cell growth/viability assays performed with C666-1, CNE-2, and HNE-1 cells demonstrate a decreased cell number in the presence of daily ribavirin treatment [black curve: ctrl (H_2O vehicle); dark gray curve: ribavirin 10 μmol/L; medium gray curve: ribavirin 20 μmol/L; light gray curve: ribavirin 50 μmol/L; *, $P < 0.05$, **, $P < 0.01$, ***, $P < 0.001$, ****, $P < 0.0001$ ribavirin vs. ctrl, $n = 3$]. **B,** Representative images of C666-1, CNE-2, and HNE-1 cells treated with ribavirin (50 μmol/L) or control for 48 hours. Scale bar, 0.5 mm.

Given that EZH2, Snail, eIF4E, and IMPDH are known to be modulated by ribavirin, we first assessed expression of these proteins in C666-1, CNE-2, and HNE-1 cells following 72 and 96 hours of ribavirin (50 μmol/L) treatment. EZH2 expression was significantly decreased in C666-1 and HNE-1 cells and trended down in CNE-2 cells after 96 hours of treatment (**Fig. 4B**). Decreased EZH2 expression also correlated with decreased EZH2 activity, as measured by a histone methyltransferase assay. This histone methyltransferase activity was significantly decreased in C666-1 (Ctrl: 100% vs. Rib10 μmol/L 35.10% vs. Rib50 μmol/L 32.79% vs. Rib100 μmol/L 5.62%) and CNE-2 (Ctrl: 100% vs. Rib10 μmol/L 39.51% vs. Rib50 μmol/L 47.75% vs. Rib100 μmol/L -22.50%) cells following treatment with ribavirin (Supplementary Fig. S4). Ribavirin therefore inhibits EZH2 activity and protein expression. We also examined the expression of EZH2's partner, Snail, and noted lower levels following 72 hours of treatment in CNE-2 cells and 96 hours of treatment in C666-1 and HNE-1 cells (**Fig. 4B**). In addition, total eIF4E and phosphorylated-eIF4E protein expression were decreased following 72 hours of ribavirin (50 μmol/L) treatment in CNE-2 cells and 96 hours of treatment in HNE-1 cells. However, total eIF4E expression was unchanged in C666-1 cells at 96 hours, while P-eIF4E was decreased following 96 hours of treatment (**Fig. 4B**). Similarly, total mTOR expression was unchanged, while P-mTOR was decreased in all cell lines following 72 hours of ribavirin (50 μmol/L) treatment (**Fig. 4B**). Furthermore, cyclin D1 was decreased in all three cell lines following 72 hours of ribavirin (50 μmol/L) treatment (**Fig. 4B**).

The last pathway we studied was the IMPDH pathway. Interestingly, IMPDH2 expression following 72 hours of ribavirin (50 μmol/L) treatment was increased in C666-1 and HNE-1 cells and trending upward in CNE-2 cells (**Fig. 4B**). While counter to our initial hypothesis, this increased expression could represent a feedback mechanism in which total IMPDH2 protein is upregulated in response to reduced enzyme activity and therefore reduced nucleotide pools. To investigate this further, we next performed an assay measuring IMPDH enzymatic activity in C666-1, CNE-2, and HNE-1 cells and found that treatment with ribavirin (50 μmol/L) led to a reduction in IMPDH activity in a cell line-dependent manner (**Fig. 4C**). Taken together with our Western blot data, these findings suggest that ribavirin inhibits IMPDH activity in NPC, which could lead to a compensatory upregulation of total protein expression. To confirm IMPDH involvement in response to ribavirin treatment, we performed a rescue experiment where CNE-2 cells were simultaneously treated with ribavirin (50 μmol/L) and guanosine (50 μmol/L), hypothesizing

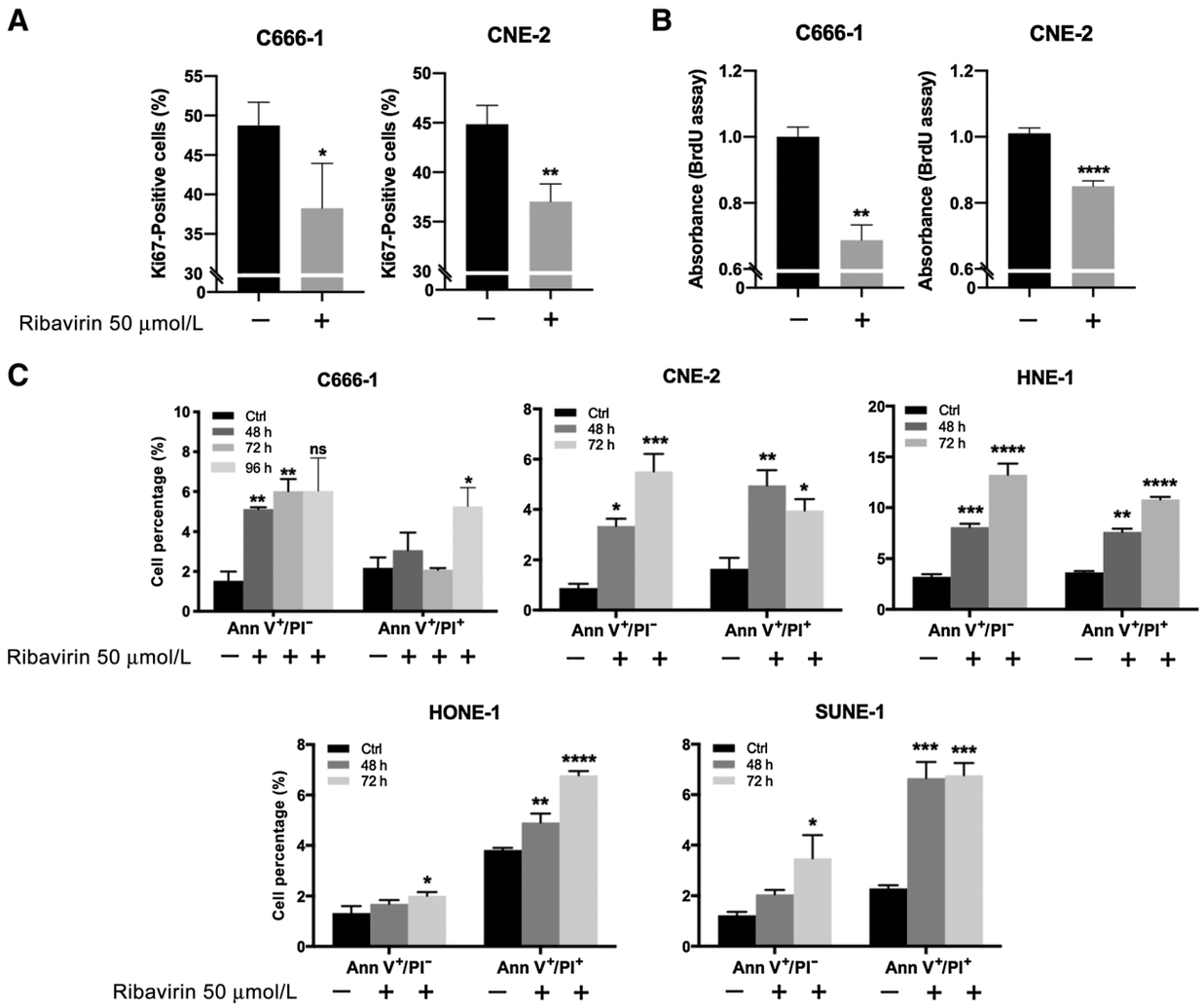

Figure 2.

Ribavirin induces NPC cell-cycle arrest and cell death. **A,** Assessment of Ki67-positive C666-1 and CNE-2 cells, using Ki67/propidium iodide (PI) staining after 48-hour daily ribavirin (50 μmol/L) treatment. Ribavirin significantly decreases the number of Ki67-positive cells, representing an increase in cell-cycle arrest (*, $P < 0.05$, **, $P < 0.01$ ribavirin vs. ctrl, $n = 3$). **B,** BrdU cell proliferation assay in C666-1 and CNE-2 cells, performed after 48-hour daily ribavirin (50 μmol/L) treatment. Ribavirin significantly decreases BrdU incorporation into C666-1 and CNE-2 cells. Data normalized to controls. (**, $P < 0.01$, ****, $P < 0.0001$ ribavirin vs. ctrl, $n = 3$). **C,** Quantification of cell death for C666-1, CNE-2, HNE-1, HONE-1, and SUNE-1 cells using flow cytometry and Annexin-V (AnnV)/PI staining 48, 72, and 96 hours (C666-1 only) after treatment. Ribavirin (50 μmol/L) significantly increases the number of $AnnV^+/PI^-$ and $AnnV^+/PI^+$ cells (*, $P < 0.05$, **, $P < 0.01$, ***, $P < 0.001$, ****, $P < 0.0001$ ribavirin vs. ctrl, $n = 3$). ns, not significant.

that repleting guanine nucleotide pools would alter the effect of ribavirin on NPC cells. We treated CNE-2 cells with ribavirin (50 μmol/L), guanosine (50 μmol/L), or both and tallied viable cells at days 2, 4, and 6 posttreatment. After 6 days, there were more cells in the ribavirin (50 μmol/L) plus guanosine (50 μmol/L) cotreatment group compared with the ribavirin (50 μmol/L)-only group (**Fig. 4D**; Supplementary Table S1). However, this rescue was only partial, as the ribavirin (50 μmol/L) plus guanosine (50 μmol/L) group still had fewer cells than the control group (**Fig. 4D**; Supplementary Table S1). These results suggest that the IMPDH pathway is affected by ribavirin in NPC but is not the only contributing mechanism. However, our data do not establish which metabolite(s) of ribavirin are active on the IMPDH pathway and they also do not demonstrate whether these effects are direct or indirect.

Ribavirin impairs tumor growth in human cell line–derived xenografts

Ribavirin has previously been shown to decrease tumor burden *in vivo* in multiple cancer models (19, 22). Therefore, we next sought to determine the impact of ribavirin treatment on two NPC xenograft models *in vivo*. We subcutaneously injected human C666-1 and CNE-2 cells into the flanks of athymic immunodeficient mice and measured tumor volumes over time with daily ribavirin (100 mg/kg) or vehicle (H_2O) control delivered via intraperitoneal injection. Treatment with ribavirin as monotherapy on day 0 led to a significant reduction in average tumor volume beginning on day 31 in the C666-1 model (Ctrl: 981.63 mm^3 vs. Rib: 424.48 mm^3; **Fig. 5A**). This difference increased further by the end of the experiment on day 38 (Ctrl: 1337.25 mm^3 vs. Rib: 583.75 mm^3),

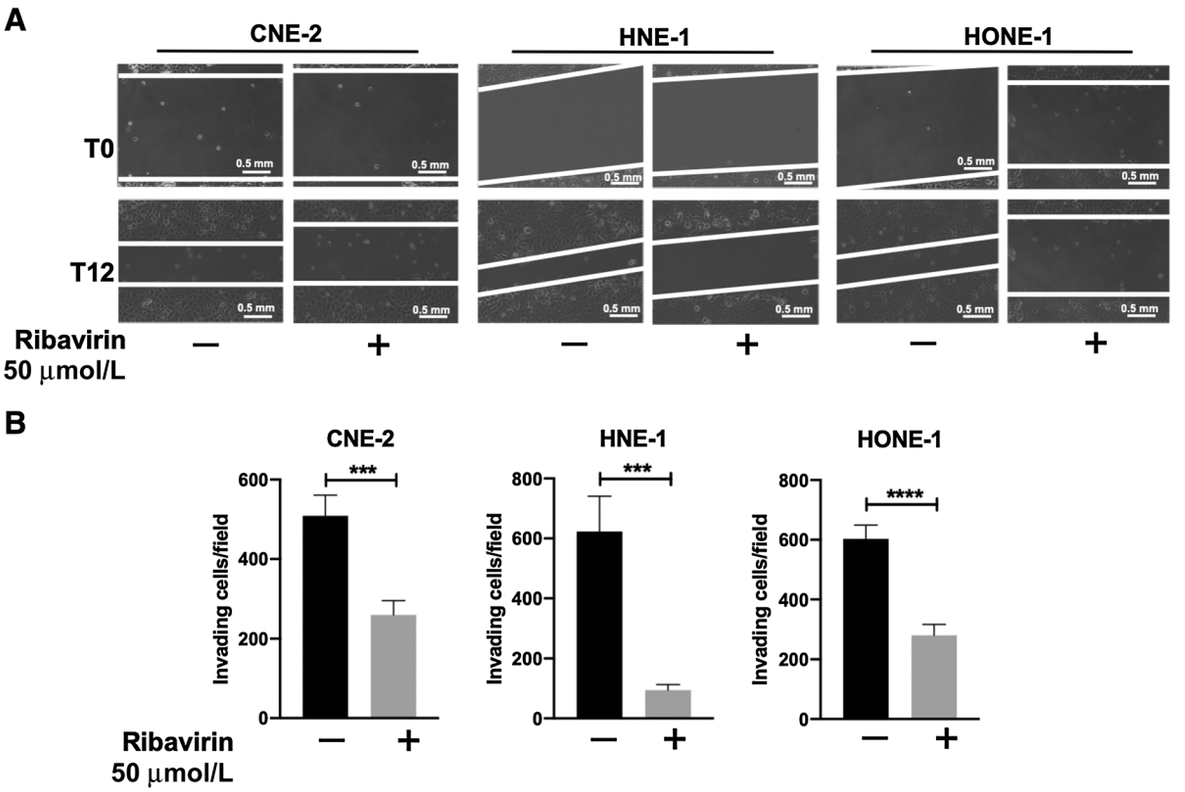

Figure 3.

Ribavirin reduces NPC cell migratory and invasive capacity. **A,** Migration of CNE-2, HNE-1, and HONE-1 cells treated with vehicle (ctrl: H_2O) or ribavirin (50 μmol/L) was assessed using the scratch wound assay. Representative photographs were taken immediately after the scratch (T0) and 12 hours later (T12). Scale bar, 0.5 mm. **B,** Invasion of CNE-2, HNE-1, and HONE-1 cells treated with vehicle or ribavirin (50 μmol/L) was assessed using inserts coated with Matrigel matrix. Ribavirin treatment significantly decreased the number of cells invading through the Matrigel matrix in all cell lines, representing a decrease in invasive capacity of NPC cells (***, $P < 0.001$; ****, $P < 0.0001$, ribavirin vs. ctrl, $n = 3$).

when vehicle-treated mice had to be euthanized. Similarly, in the CNE-2 model, treatment with ribavirin (100 mg/kg) on day 4 led to a significant reduction in average tumor volume beginning on day 14 (Ctrl: 1,167.24 mm^3 vs. Rib: 421.94 mm^3) and further increasing by the end of the experiment on day 18 (Ctrl: 1757.04 mm^3 vs. Rib: 782.59 mm^3; **Fig. 5B**). Following sacrifice, we resected flank tumors for qualitative analysis. Imaging tumor sections demonstrated qualitatively decreased tumor size in both xenograft models (Supplementary Fig. S5A). Resected tumors were stained with hematoxylin and eosin as well as IHC staining for cleaved caspase-3 (**Fig. 5C**). A 3-fold increase in cleaved caspase-3–positive cells was observed in tumors from ribavirin-treated animals compared with controls (Ctrl: 1.87% cells/field vs. Rib: 6.14% cells/field, $P < 0.01$), illustrating increased apoptosis in the presence of ribavirin *in vivo* (**Fig. 5C** and **D**).

Ribavirin enhances the effects of radiation in NPC

XRT is a central component of the standard treatment regimen for NPC (1). Given that ribavirin is known to enhance the cytotoxic effects of radiotherapy (19), we next investigated the effects of combining ribavirin with radiation for NPC. We first performed a clonogenic cell survival assay in C666-1 and CNE-2 cells with ribavirin treatment (25 μmol/L) followed by XRT 4 hours later. Given their relative radioresistance, CNE-2 cells were treated with higher doses of radiation than C666-1 cells. Fewer cell colonies remained following treatment with ribavirin or radiation monotherapy compared with controls (**Fig. 6A** and **B**). Furthermore, combination therapy resulted in fewer colonies compared with either treatment alone in both cell lines (**Fig. 6A** and **B**). In addition, at multiple doses of radiation, a significant reduction in the surviving fraction of cells was seen following treatment with ribavirin plus radiation in both C666-1 cells (0.5 Gy 66.00% vs. Rib25 μmol/L + 0.5 Gy 28.00%; 2 Gy 11.00% vs. Rib25 μmol/L + 2 Gy 6.67%) and CNE-2 cells (6 Gy 57.33% vs. Rib25 μmol/L + 6 Gy 33.33%; 8 Gy 32.33% vs. Rib25 μmol/L + 8 Gy 18.67%; **Fig. 6C** and **D**). Flow cytometry analysis showed that when we combined radiation with ribavirin for 72 hours, we increased the total number of $AnnV^+$ cells compared with either treatment alone in both C666-1 (XRT: 39.33% vs. Rib + XRT: 51.33%) and CNE-2 (XRT: 22.15% vs. Rib + XRT: 32.63%) cells (**Fig. 6E** and **F**). Moreover, we also increased the total number of cells staining positive for both AnnV and PI in C666-1 (XRT: 23.53% vs. Rib + XRT: 34.00%) and CNE-2 (XRT: 18.30% vs. Rib + XRT: 26.30%) cells (**Fig. 6E** and **F**). On the basis of these promising data *in vitro*, we investigated the effects of combining ribavirin with XRT *in vivo* in a CNE-2 flank tumor model. Animals were treated with daily ribavirin (100 mg/kg), vehicle (H_2O) control, XRT (5 Gy over 3 fractions), or the combination of ribavirin + XRT. The combination of ribavirin pretreatment and XRT led to a significant reduction in flank tumor volume compared with either ribavirin or XRT alone at the end of the experiment on day 21 (Ctrl: 1856.7 mm^3

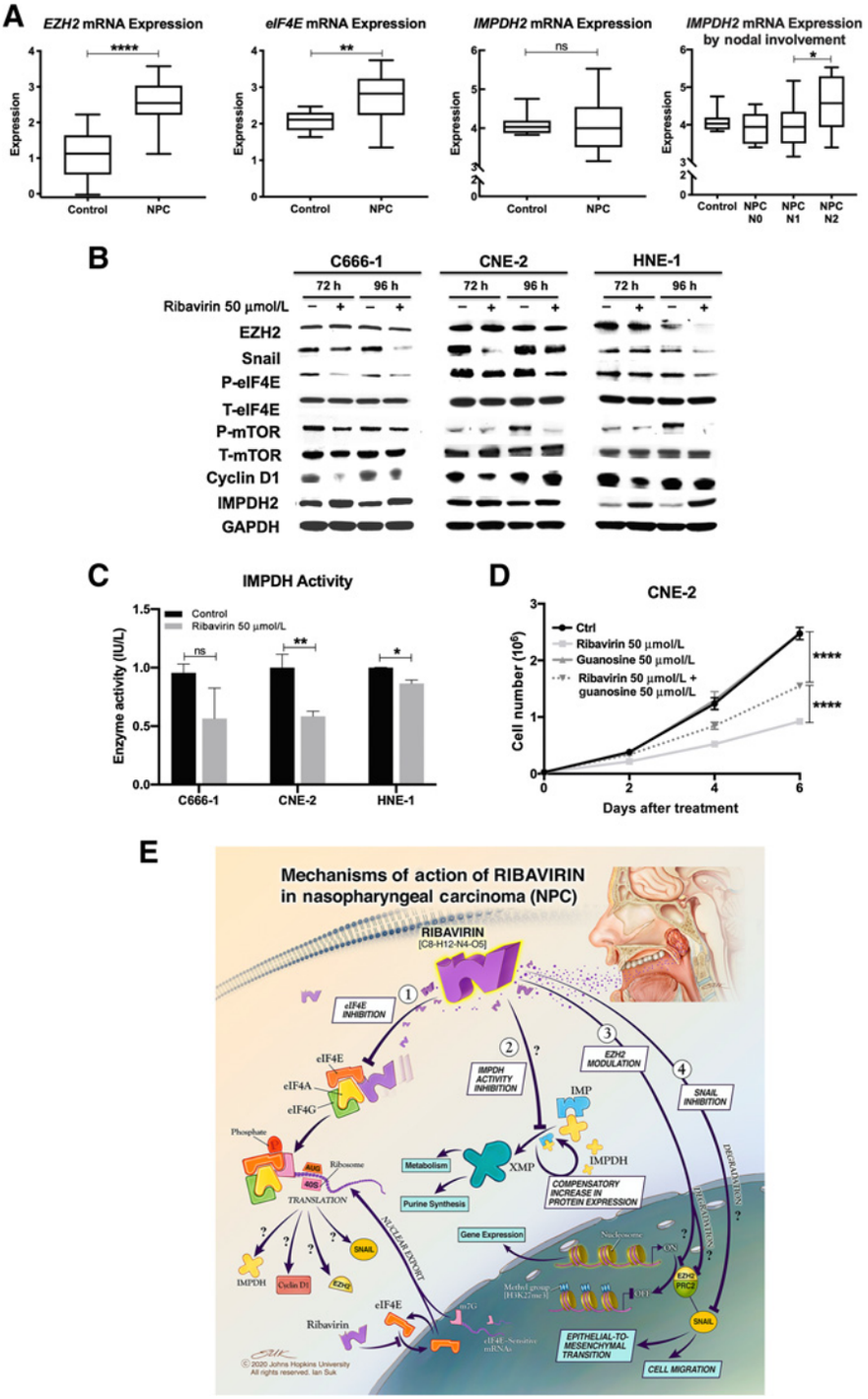

Figure 4.

Potential mechanisms of action of ribavirin in NPC. **A,** Sengupta and colleagues' (24) genomic dataset indicating expression of *EZH2, eIF4E*, and *IMPDH2* in human NPC ($n = 31$) and normal adjacent nasopharynx samples ($n = 10$). *EZH2* and *eIF4E* expressions were significantly elevated in NPC compared with normal adjacent tissue. Increased *IMPDH2* mRNA expression was present in NPC samples with greater lymph node involvement by TNM staging (ns, not statistically significant; *, $P < 0.05$; **, $P < 0.01$; ***, $P < 0.001$; ****, $P < 0.0001$; ribavirin vs. ctrl). **B,** Western blot analyses of EZH2, Snail, total and phospho-eIF4E, total and phospho-mTOR, cyclin D1, and IMPDH2 in C666-1, CNE-2, and HNE-1 cells after 72 and 96 hours of ribavirin (50 μmol/L) treatment. Ribavirin decreases expression of EZH2, Snail, total and phospho-eIF4E, cyclin D1, and phospho-mTOR in a time- and cell line–dependent manner. Protein expression of IMPDH2 following ribavirin (50 μmol/L) treatment was increased in C666-1 and HNE-1 cells and trending upward in CNE-2 cells after 72 hours. **C,** IMPDH activity assay revealed that ribavirin (50 μmol/L) decreases IMPDH enzymatic activity in a cell line–dependent manner, including a nonsignificant reduction in C666-1 cells and statistically significant reduction in CNE-2 and HNE-1 cells. Data normalized to controls (ns, not statistically significant; *, $P < 0.05$; **, $P < 0.01$; ribavirin vs. ctrl, $n = 3$). **D,** Addition of guanosine (50 μmol/L) partially rescued the inhibitory effects of ribavirin on cellular growth/ viability in CNE-2 cells (****, $P < 0.0001$; ribavirin vs. ctrl, $n = 3$). **E,** Schematic by I. Suk representing potential mechanisms of action of ribavirin in NPC cells.

vs. Rib: 725.8 mm^3 vs. XRT: 839.9 mm^3 vs. Rib + XRT: 416.4 mm^3; **Fig. 6G**; Supplementary Fig. S5B). Taken together, our data show that ribavirin enhances the effects of radiation on NPC *in vitro* and *in vivo*.

Discussion

NPC is a head and neck cancer with poor prognosis whose hallmark is EBV positivity (26). Standard of care includes radiation, antimetabolites, and platinum-based therapies with considerable toxicity. There is a notable lack of targeted therapies for NPC despite knowledge of multiple promising protein targets with central, well-defined roles in this cancer, including EZH2, Snail, eIF4E, and IMPDH. These proteins may be particularly important in late-stage and recurrent NPC, the areas of greatest unmet need. We found that modulating these proteins with ribavirin had a potent anti-tumor effect. *In vitro*, ribavirin decreased cell proliferation, reduced migration and invasion,

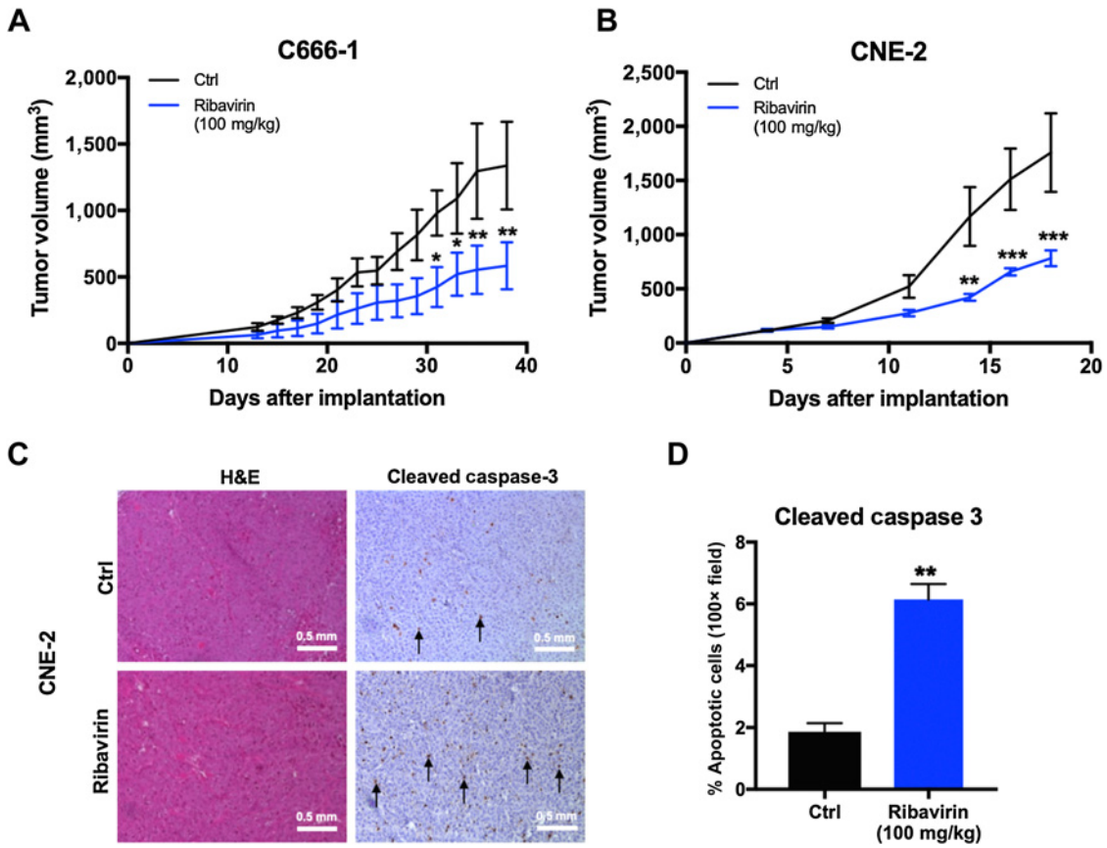

Figure 5.

Ribavirin impairs NPC tumor growth *in vivo*. **A** and **B,** Average flank tumor xenograft volumes from immunodeficient mice subcutaneously implanted with C666-1 or CNE-2 cells and treated with daily ribavirin (100 mg/kg) or vehicle control. Ribavirin treatment significantly decreased tumor volume compared with controls. **C** and **D,** H&E and cleaved caspase-3 stainings performed on CNE-2 tumors resected on day 18. Ribavirin-treated tumors exhibit increased positive staining for cleaved caspase-3 compared with vehicle-treated controls. Scale bar, 0.5 mm (*, $P < 0.05$; **, $P < 0.01$; ***, $P < 0.001$, ribavirin vs. ctrl).

promoted cell-cycle arrest and cell death, and sensitized to therapy with radiation. *In vivo*, it reduced flank tumor growth both as monotherapy and in combination with radiation.

An early, fundamental step in the pathogenesis of NPC is establishment of persistent EBV infection in nasopharyngeal epithelium (26). Cyclin D1, a cell-cycle regulatory protein involved in the G_1–S transition, is overexpressed in NPC and known to directly facilitate EBV infection (27). Cyclin D1 is posttranscriptionally regulated by eIF4E (28), and eIF4E inhibition by ribavirin is consequently known to reduce protein levels of cyclin D1 (28). Our mechanistic data align with these prior studies. This effect may partly explain NPC cell-cycle arrest in G_0 following four to six days of ribavirin treatment–a timeline consistent with previously reported data in brain tumors (19, 22). Thus, while ribavirin does not appear to directly impact EBV replication, it may potentially create an environment less receptive to EBV infection and indirectly decrease the risk of developing recurrent or metastatic NPC.

While outcomes for early-stage NPC are generally good, there is a significant unmet need in addressing treatment failure and advanced-stage disease, which affect nearly half of the patients with NPC (7). The primary driver of treatment failure is NPC's proclivity for systemic dissemination (5), rendering ribavirin's antimigratory and anti-invasive effects particularly compelling. Our scratch wound and invasion assay data are consistent with ribavirin's documented ability to decrease migration, invasion, and adhesion in other cancers. Prior work in breast cancer and glioblastoma suggests that these effects may be mediated by inhibition of MMP-3 and MMP-9 (19, 20); additional work in cervical cancer demonstrated reduced gelatinolytic activity following ribavirin treatment, suggesting decreased activity of MMP-2 and MMP-9 (29). Complementing these studies, we show that ribavirin's effects on NPC migration and invasion may be mediated, in part, by inhibition of EZH2 and Snail, a pathway consistent with previously published work (19, 22). In addition to regulating differentiation, cell-cycle progression, and apoptosis, EZH2 is also associated with higher risk of relapse, invasiveness, and metastasis in NPC (9). Prior studies have demonstrated that EZH2 silences E-cadherin, thus enabling metastasis, through methylation of H3K27 (30). In NPC, this silencing requires EZH2 to complex with Snail, a transcription factor that mediates tumor progression and metastasis (10). Snail has been identified as a potential target for late-stage patients, although, to date, neither EZH2 nor Snail have been pharmacologically targeted in NPC (13).

Ribavirin's anticancer effects in rapidly growing NPC cells may also be driven by its interaction with IMPDH2, an isoform of IMPDH linked to malignant transformation, and subsequent depletion of guanine nucleotide pools (31). Elevated IMPDH2 expression is known

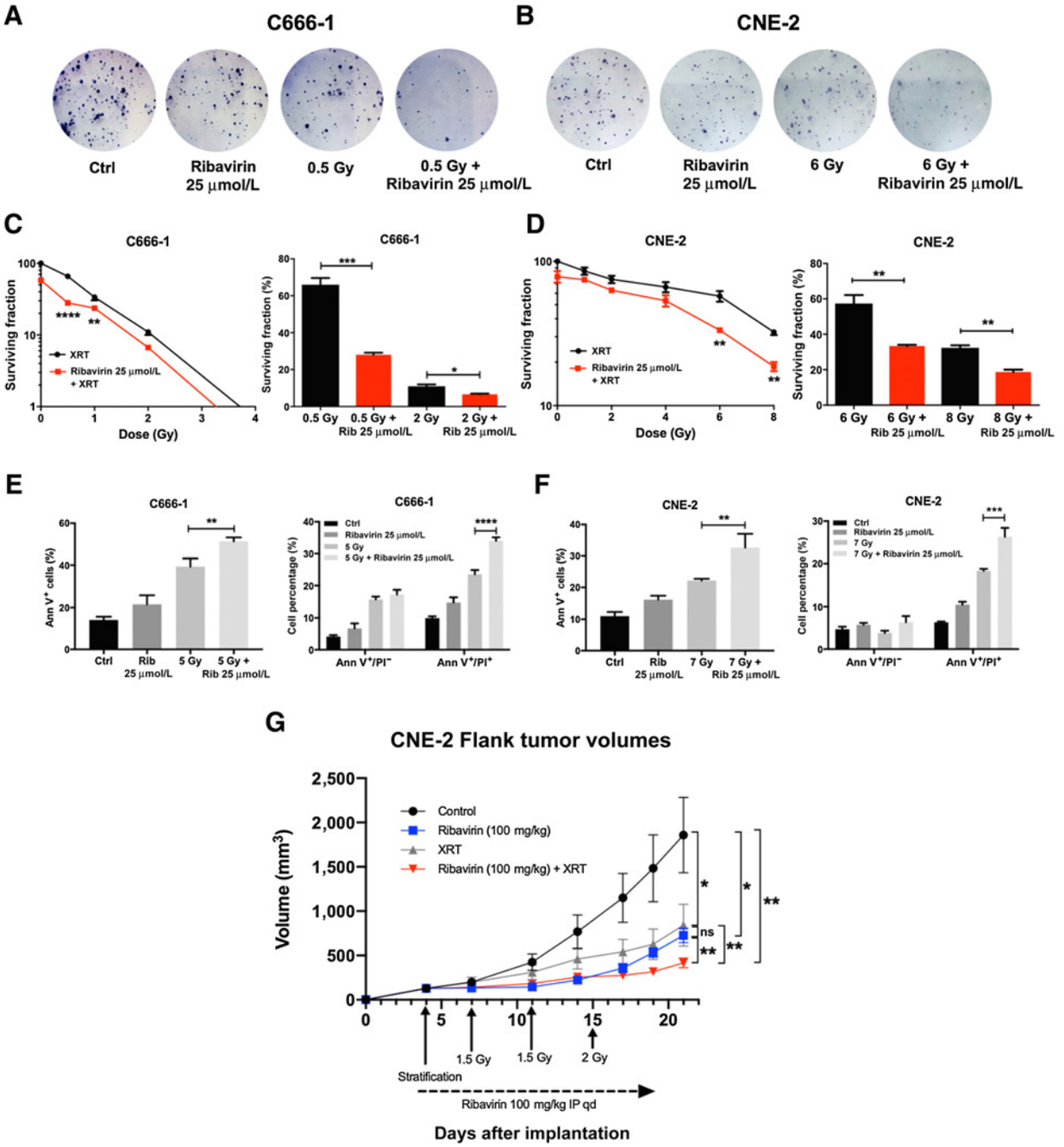

Figure 6.

Ribavirin enhances the efficacy of radiation therapy in NPC *in vitro* and *in vivo*. Representative photographs from clonogenic assays with C666-1 cells (**A**) and CNE-2 cells (**B**) following treatment with ctrl, 25 μmol/L ribavirin, radiation (XRT; C666-1: 0.5 Gy; and CNE-2: 6 Gy), or ribavirin + XRT. Ribavirin + XRT led to a decreased number of colonies compared with either treatment alone in both cell lines. Quantification of clonogenic assay, counting C666-1 (**C**) and CNE-2 (**D**) colonies (>50 cells) following treatment with 25 μmol/L ribavirin and various doses of XRT. Ribavirin + XRT led to fewer colonies compared with XRT alone. Quantification of cell death for C666-1 (**E**) and CNE-2 (**F**) cells using flow cytometry and AnnV/PI staining 72 hours after treatment with 25 μmol/L ribavirin and XRT (C666-1: 5 Gy and CNE-2: 7 Gy). Ribavirin + XRT led to a significant increase in the number of $AnnV^+$ cells and $AnnV^+/PI^+$ cells compared with either treatment alone in both cell lines. **G,** Average flank tumor xenograft volumes from immunodeficient mice subcutaneously implanted with CNE-2 cells and treated with vehicle control, daily (qd) ribavirin (100 mg/kg), XRT (3 fractions), or daily ribavirin (100 mg/kg) + XRT. Ribavirin potentiated the effects of radiation therapy *in vivo*, demonstrated by a reduction in flank tumor volume in the combination therapy group compared with treatment with either ribavirin or XRT alone (ns, not statistically significant; *, $P < 0.05$; **, $P < 0.01$; ***, $P < 0.001$; ****, $P < 0.0001$, ribavirin vs. ctrl).

to correlate with tumor-node-metastasis (TNM) stage and distant metastasis in NPC and is an independent prognostic factor for overall survival and disease-free survival (16). Unexpectedly, we found that treatment of NPC cells with ribavirin led to increased IMPDH2 protein expression but decreased enzymatic activity. This could potentially result from a feedback mechanism as described in leukemia and melanoma cells, in which *IMPDH* gene expression is upregulated due to reduced nucleotide pool availability (32, 33). Providing guanosine partially rescued ribavirin's inhibitory effect on cell proliferation, suggesting that IMPDH2 may be a key mediator of ribavirin's anticancer effects in NPC, although it is not the sole mechanism underlying these actions. Ultimately, it is not known whether ribavirin's effects on IMPDH are direct or indirect in NPC and which metabolites [ribavirin monophosphate (RMP), ribavirin triphosphate (RTP), or ribavirin diphosphate (RDP)] of ribavirin are promoting this activity. Previous studies linking IPMDH activity to ribavirin were conducted using purified RMP and IMPDH; given that RMP is not a major ribavirin metabolite in human cellular systems, it would be somewhat unexpected if RMP were the metabolite present and active in NPC (34). Future studies are clearly needed to better characterize this mechanistic pathway in NPC.

eIF4E may ultimately be a common downstream effector of these pathways, given its central role in translation initiation. eIF4E is overexpressed in NPC, and its phosphorylation promotes broad protumorigenic functions, including expression of growth signals, modeling the extracellular matrix, promoting cellular proliferation, and inhibiting apoptosis (19). eIF4E is also known to increase resistance to gemcitabine and cisplatin, foundations of current NPC chemotherapy (35, 36). Ribavirin's inhibition of eIF4E was first tested clinically in acute myeloid leukemia (37) and has since been documented in many malignancies (18, 20, 22, 28, 37–40) and may play a central role in our observed anticancer effects in NPC; it could potentially help overcome resistance to currently used therapies, as demonstrated in a recent study in NPC (41). Inhibition of eIF4E may also be a critical mediator of increasing NPC radiosensitivity to ribavirin; our clonogenic assay and *in vivo* data align with prior work demonstrating that eIF4E is a key target for tumor cell radiosensitization at the level of translational control of gene expression in multiple cancer cell lines (42). Finally, given the close link between eIF4E and mTOR, and mTOR's known importance in NPC cell proliferation and stem cell properties (43), we investigated the effect of ribavirin on mTOR in NPC and found that it decreased levels of phosphorylated mTOR, complementing our mechanistic data involving the mTOR/eIF4E axis and aligning with prior literature (39).

A clear clinical advantage of ribavirin is its ability to simultaneously modulate multiple proteins with central regulatory roles in cancer. It is well accepted that targeting multiple pathways in this manner improves treatment efficacy and prevents the emergence of treatment resistance. In addition to modulating key pathways, ribavirin is particularly well suited for clinical evaluation as an adjuvant therapy in NPC due to its ability to improve the efficacy of current standard-of-care therapies: radiation, gemcitabine, and cisplatin. Here, we demonstrate that ribavirin sensitizes NPC to the effects of radiation, an effect also seen in cancers of the breast and brain (19, 42). One study documented synergistic activity of ribavirin and gemcitabine against enteroviruses (44), and prior oncology literature shows that targeting eIF4E increases sensitivity to gemcitabine in lung and pancreatic cancer (45, 46). Ribavirin's inhibition of eIF4E has also been shown to increase sensitivity to cisplatin in ovarian cancer and 5-FU (a former staple of NPC chemotherapy) in NPC (40, 41). Notably, ribavirin is the only FDA-approved drug with documented activity against eIF4E.

Given that ribavirin has been used extensively to treat hepatitis C, its dosing parameters are well-studied, with its main toxicity being a reversible hemolytic anemia. Adult patients undergoing treatment for hepatitis C receive 800–1,200 mg/day for up to 48 weeks, while patients with cancer have received up to 2,800 mg/day without toxicity (18, 47). In an AML trial, patients with clinical responses to treatment involving ribavirin had median plasma levels of 33 μmol/L (18). In another study, patients with subacute sclerosing panencephalitis achieved and tolerated serum concentrations of approximately 85 μmol/L following 30 mg/kg oral ribavirin (48). Our *in vitro* and *in vivo* data demonstrate therapeutic efficacy at doses well below these clinical thresholds. We used a dose of 100 mg/kg/day in our *in vivo* experiments based on a prior maximally tolerated dose study performed in our laboratory as well as published models in breast and cervical cancer (20, 29). This corresponds to a human dose of approximately 500 mg/day for a 60 kg patient. Our *in vitro* data demonstrated strong responses to ribavirin at doses of 10 μmol/L, 20 μmol/L, and 50 μmol/L in multiple cell lines. Thus, our data reflect doses that are clinically achievable in humans and considerably lower than therapeutically useful doses for antiviral and anticancer applications. Ribavirin is also known to decrease the dose needed of other chemotherapeutic drugs, including a documented 1,000-fold decrease in the effective dose of cytarabine in AML (18). Ribavirin is also being studied clinically in combination therapy regimens in oropharyngeal squamous cell carcinoma (NCT01721525; ref. 49), metastatic breast cancer (NCT01056757), hepatocellular carcinoma (NCT00375661, NCT00834860, NCT02771405), lymphoma (NCT02717949, NCT03585725), and prostate cancer [UMIN000012521 (50), UMIN000021107]. We note that in some cases, these tumors are driven by ribavirin-sensitive viruses (i.e., hepatitis B virus and human papillomavirus), although EBV is not directly sensitive to ribavirin. However, as discussed above, ribavirin may have indirect effects on receptivity to EBV infection.

Limitations of our study include an incompletely understood mechanism of ribavirin and the need to determine the relative importance of each pathway discussed in NPC as well as the relative potency of ribavirin's effect on each pathway. We also note that, while the clinical case for ribavirin testing in NPC is strengthened by its existing regulatory approval and safety profile, there is a lack of robust phase III data demonstrating efficacy of ribavirin in cancer. Future studies should investigate different combination therapy regimens using ribavirin with currently available treatments in NPC in both preclinical and clinical settings.

In conclusion, we provide *in vitro* and *in vivo* evidence that ribavirin represents a promising potential therapy against NPC. It fills a conspicuous gap in available targeted therapies for this cancer and is a logical choice given its modulation of prognostic proteins central to NPC cancer biology. Ribavirin may be particularly appealing in preventing and treating recurrent and late-stage NPC, the areas of greatest clinical need, especially in combination with chemo/radiotherapies. Ultimately, our study provides a foundation for clinical evaluation of ribavirin as a safe and promising step forward in the treatment of NPC.

Disclosure of Potential Conflicts of Interest

W. Ishida is a consultant/advisory board member for CortiTech. H. Brem is a consultant at AsclepiX Therapeutics, StemGen, InSightec, Accelerating Combination Therapies, Camden Partners, LikeMinds, Inc., Galen Robotics, Inc. Nurami Medical, reports receiving a commercial research grant from Arbor Pharmaceuticals, Bristol-Myers Squibb, and AcuityBio Corp., and has ownership interest (including patents) in Accelerating Combination Therapies, LLC. B. Tyler has ownership interest (including patents) in Accelerating Combination Therapeutics, LLC. No potential conflicts of interests were disclosed by the other authors.

Authors' Contributions

S. Huq: Conceptualization, methodology, data curation, formal analysis, writing-original draft, writing-review and editing. **J. Casaos:** Conceptualization, methodology, data curation, formal analysis, writing-original draft, writing-review and editing, project administration, study supervision. **R. Serra:** Methodology, data curation, formal analysis. **M. Peters:** Data curation, formal analysis, writing-original draft, writing-review and editing. **Y. Xia:** Methodology, data curation, writing-original draft, writing-review and editing. **A.S. Ding:** Conceptualization, methodology, data curation, formal analysis. **J. Ehresman:** Methodology, data curation. **J.N. Kedda:** Data curation. **M. Morales:** Conceptualization, methodology, formal analysis, writing-original draft, writing-review and editing, project administration. **N.L. Gorelick:** Conceptualization, formal analysis, writing-original draft, writing-review and editing. **T. Zhao:** Methodology, formal analysis, writing-original draft, writing-review and editing. **W. Ishida:** Writing-original draft, writing-review and editing. **A. Perdomo-Pantoja:** Data curation, writing-original draft, writing-review and editing. **A. Cecia:** Data curation. **C. Ji:** Data curation. **I. Suk:** Project administration. **D. Sidransky:** Data curation, writing-original draft, writing-review and editing. **M. Brait:** Data curation, formal analysis, writing-original draft, writing-review and editing. **H. Brem:** Writing-original draft, writing-review and editing, study supervision. **N. Skuli:** Conceptualization, formal analysis, writing-original draft, writing-review and editing. **B. Tyler:** Methodology, formal analysis, writing-original draft, writing-review and editing, study supervision.

Acknowledgments

Cell lines were kindly provided by the Head and Neck Cancer Research Laboratory and Ambinder Laboratory at Johns Hopkins with permission from Qian Tao (Chinese University of Hong Kong) and Maria Lung (University of Hong Kong). We thank Simy Buckwold, Rajani Ravi, Yoshikuni Inokawa, and Daria Gaykalova for assistance with obtaining and culturing cells, and the Hunterian Neurosurgical Research Laboratory for helpful comments and editing. This work was supported by a Carolyn Kuckein Student Research Fellowship from Alpha Omega Alpha (to S. Huq) and Medical Student Research Fellowships from the Howard Hughes Medical Institute (to J. Casaos and Y. Xia).

The costs of publication of this article were defrayed in part by the payment of page charges. This article must therefore be hereby marked *advertisement* in accordance with 18 U.S.C. Section 1734 solely to indicate this fact.

Received June 5, 2019; revised December 9, 2019; accepted June 9, 2020; published first June 30, 2020.

References

1. Chua MLK, Wee JTS, Hui EP, Chan ATC. Nasopharyngeal carcinoma. Lancet North Am Ed 2016;387:1012–24.
2. Dickson RI, Flores AD. Nasopharyngeal carcinoma: an evaluation of 134 patients treated between 1971–1980. Laryngoscope 1985;95:276–83.
3. Buell P. The effect of migration on the risk of nasopharyngeal cancer among Chinese. Cancer Res 1974;34:1189–91.
4. Chua MLK, Chan ATC. Gemcitabine: a game changer in nasopharyngeal carcinoma. Lancet North Am Ed 2016;388:1853–4.
5. Zhang L, Huang Y, Hong S, Yang Y, Yu G, Jia J, et al. Gemcitabine plus cisplatin versus fluorouracil plus cisplatin in recurrent or metastatic nasopharyngeal carcinoma: a multicentre, randomised, open-label, phase 3 trial. Lancet 2016; 388:1883–92.
6. Lee AW, Ma BB, Ng WT, Chan AT. Management of nasopharyngeal carcinoma: current practice and future perspective. J Clin Oncol 2015;33:3356–64.
7. Wei WI, Kwong DL. Current management strategy of nasopharyngeal carcinoma. Clin Exp Otorhinolaryngol 2010;3:1–12.
8. Kim KH, Roberts CW. Targeting EZH2 in cancer. Nat Med 2016;22:128–34.
9. Alajez NM, Shi W, Hui AB, Bruce J, Lenarduzzi M, Ito E, et al. Enhancer of Zeste homolog 2 (EZH2) is overexpressed in recurrent nasopharyngeal carcinoma and is regulated by miR-26a, miR-101, and miR-98. Cell Death Dis 2010;1:e85.
10. Tong ZT, Cai MY, Wang XG, Kong LL, Mai SJ, Liu YH, et al. EZH2 supports nasopharyngeal carcinoma cell aggressiveness by forming a co-repressor complex with HDAC1/HDAC2 and Snail to inhibit E-cadherin. Oncogene 2012;31: 583–94.
11. Hwang CF, Huang HY, Chen CH, Chien CY, Hsu YC, Li CF, et al. Enhancer of zeste homolog 2 overexpression in nasopharyngeal carcinoma: an independent poor prognosticator that enhances cell growth. Int J Radiat Oncol Biol Phys 2012; 82:597–604.
12. Herranz N, Pasini D, Diaz VM, Franci C, Gutierrez A, Dave N, et al. Polycomb complex 2 is required for E-cadherin repression by the Snail1 transcription factor. Mol Cell Biol 2008;28:4772–81.
13. Luo WR, Li SY, Cai LM, Yao KT. High expression of nuclear Snail, but not cytoplasmic staining, predicts poor survival in nasopharyngeal carcinoma. Ann Surg Oncol 2012;19:2971–9.
14. Zhang P, Wu SK, Wang Y, Fan ZX, Li CR, Feng M, et al. p53, MDM2, eIF4E and EGFR expression in nasopharyngeal carcinoma and their correlation with clinicopathological characteristics and prognosis: a retrospective study. Oncol Lett 2015;9:113–8.
15. Borden KL, Culjkovic-Kraljacic B. Ribavirin as an anti-cancer therapy: acute myeloid leukemia and beyond? Leuk Lymphoma 2010;51:1805–15.
16. Xu Y, Zheng Z, Gao Y, Duan S, Chen C, Rong J, et al. High expression of IMPDH2 is associated with aggressive features and poor prognosis of primary nasopharyngeal carcinoma. Sci Rep 2017;7:745.
17. Casaos J, Gorelick NL, Huq S, Choi J, Xia Y, Serra R, et al. The use of ribavirin as an anticancer therapeutic: will it go viral? Mol Cancer Ther 2019;18:1185–94.
18. Assouline S, Culjkovic-Kraljacic B, Bergeron J, Caplan S, Cocolakis E, Lambert C, et al. A phase I trial of ribavirin and low-dose cytarabine for the treatment of relapsed and refractory acute myeloid leukemia with elevated eIF4E. Haematologica 2014;100:e7–9.
19. Volpin F, Casaos J, Sesen J, Mangraviti A, Choi J, Gorelick N, et al. Use of an antiviral drug, ribavirin, as an anti-glioblastoma therapeutic. Oncogene 2017;36: 3037–47.
20. Pettersson F, Del Rincon SV, Emond A, Huor B, Ngan E, Ng J, et al. Genetic and pharmacologic inhibition of eIF4E reduces breast cancer cell migration, invasion, and metastasis. Cancer Res 2015;75:1102–12.
21. Pettersson F, Yau C, Dobocan MC, Culjkovic-Kraljacic B, Retrouvey H, Puckett R, et al. Ribavirin treatment effects on breast cancers overexpressing eIF4E, a biomarker with prognostic specificity for luminal B-type breast cancer. Clin Cancer Res 2011;17:2874–84.
22. Casaos J, Huq S, Lott T, Felder R, Choi J, Gorelick N, et al. Ribavirin as a potential therapeutic for atypical teratoid/rhabdoid tumors. Oncotarget 2018;9:8054–67.
23. Tan J, Ye J, Song M, Zhou M, Hu Y. Ribavirin augments doxorubicin's efficacy in human hepatocellular carcinoma through inhibiting doxorubicin-induced eIF4E activation. J Biochem Mol Toxicol 2018;32:e22007.
24. Sengupta S, den Boon JA, Chen IH, Newton MA, Dahl DB, Chen M, et al. Genome-wide expression profiling reveals EBV-associated inhibition of MHC class I expression in nasopharyngeal carcinoma. Cancer Res 2006;66:7999–8006.
25. Munshi A, Hobbs M, Meyn RE. Clonogenic cell survival assay. Methods Mol Med 2005;110:21–8.
26. Raab-Traub N. Epstein-Barr virus in the pathogenesis of NPC. Semin Cancer Biol 2002;12:431–41.
27. Tsang CM, Yip YL, Lo KW, Deng W, To KF, Hau PM, et al. Cyclin D1 overexpression supports stable EBV infection in nasopharyngeal epithelial cells. Proc Natl Acad Sci U S A 2012;109:E3473–82.
28. Kentsis A, Topisirovic I, Culjkovic B, Shao L, Borden KL. Ribavirin suppresses eIF4E-mediated oncogenic transformation by physical mimicry of the 7-methyl guanosine mRNA cap. Proc Natl Acad Sci U S A 2004;101:18105–10.
29. Sharma S, Baksi R, Agarwal M. Repositioning of anti-viral drugs as therapy for cervical cancer. Pharmacol Rep 2016;68:983–9.
30. Cao Q, Yu J, Dhanasekaran SM, Kim JH, Mani RS, Tomlins SA, et al. Repression of E-cadherin by the polycomb group protein EZH2 in cancer. Oncogene 2008; 27:7274–84.
31. Nagai M, Natsumeda Y, Konno Y, Hoffman R, Irino S, Weber G. Selective upregulation of type II inosine 5'-monophosphate dehydrogenase messenger RNA expression in human leukemias. Cancer Res 1991;51:3886–90.
32. Glesne DA, Collart FR, Huberman E. Regulation of IMP dehydrogenase gene expression by its end products, guanine nucleotides. Mol Cell Biol 1991;11: 5417–25.
33. Vethe NT, Bremer S, Bergan S. IMP dehydrogenase basal activity in MOLT-4 human leukaemia cells is altered by mycophenolic acid and 6-thioguanosine. Scand J Clin Lab Invest 2008;68:277–85.

34. Streeter DG, Witkowski JT, Khare GP, Sidwell RW, Bauer RJ, Robins RK, et al. Mechanism of action of 1- -D-ribofuranosyl-1,2,4-triazole-3-carboxamide (Virazole), a new broad-spectrum antiviral agent. Proc Natl Acad Sci U S A 1973;70:1174–8.
35. Adesso L, Calabretta S, Barbagallo F, Capurso G, Pilozzi E, Geremia R, et al. Gemcitabine triggers a pro-survival response in pancreatic cancer cells through activation of the MNK2/eIF4E pathway. Oncogene 2013;32:2848–57.
36. Martinez A, Sese M, Losa JH, Robichaud N, Sonenberg N, Aasen T, et al. Phosphorylation of eIF4E confers resistance to cellular stress and DNA-damaging agents through an interaction with 4E-T: a rationale for novel therapeutic approaches. PLoS One 2015;10:e0123352.
37. Assouline S, Culjkovic B, Cocolakis E, Rousseau C, Beslu N, Amri A, et al. Molecular targeting of the oncogene eIF4E in acute myeloid leukemia (AML): a proof-of-principle clinical trial with ribavirin. Blood 2009;114:257–60.
38. Urtishak KA, Wang LS, Culjkovic-Kraljacic B, Davenport JW, Porazzi P, Vincent TL, et al. Targeting EIF4E signaling with ribavirin in infant acute lymphoblastic leukemia. Oncogene 2019;38:2241–62.
39. Dai D, Chen H, Tang J, Tang Y. Inhibition of mTOR/eIF4E by anti-viral drug ribavirin effectively enhances the effects of paclitaxel in oral tongue squamous cell carcinoma. Biochem Biophys Res Commun 2017;482:1259–64.
40. Jin J, Xiang W, Wu S, Wang M, Xiao M, Deng A. Targeting eIF4E signaling with ribavirin as a sensitizing strategy for ovarian cancer. Biochem Biophys Res Commun 2019;510:580–6.
41. Hu Z, Zhen L, Li Q, Han Q, Hua Q. Ribavirin sensitizes nasopharyngeal carcinoma to 5-fluorouracil through suppressing 5-fluorouracil-induced ERK-dependent-eIF4E activation. Biochem Biophys Res Commun 2019;513:862–8.
42. Hayman TJ, Williams ES, Jamal M, Shankavaram UT, Camphausen K, Tofilon PJ. Translation initiation factor eIF4E is a target for tumor cell radiosensitization. Cancer Res 2012;72:2362–72.
43. Yang C, Zhang Y, Zhang Y, Zhang Z, Peng J, Li Z, et al. Downregulation of cancer stem cell properties via mTOR signaling pathway inhibition by rapamycin in nasopharyngeal carcinoma. Int J Oncol 2015;47:909–17.
44. Kang H, Kim C, Kim DE, Song JH, Choi M, Choi K, et al. Synergistic antiviral activity of gemcitabine and ribavirin against enteroviruses. Antiviral Res 2015;124:1–10.
45. Thumma SC, Jacobson BA, Patel MR, Konicek BW, Franklin MJ, Jay-Dixon J, et al. Antisense oligonucleotide targeting eukaryotic translation initiation factor 4E reduces growth and enhances chemosensitivity of non-small-cell lung cancer cells. Cancer Gene Ther 2015;22:396–401.
46. Jacobson BA, Thumma SC, Jay-Dixon J, Patel MR, Dubear Kroening K, Kratzke MG, et al. Targeting eukaryotic translation in mesothelioma cells with an eIF4E-specific antisense oligonucleotide. PLoS One 2013;8:e81669.
47. Abenavoli L, Mazza M, Almasio PL. The optimal dose of ribavirin for chronic hepatitis C: from literature evidence to clinical practice: the optimal dose of ribavirin for chronic hepatitis C. Hepat Mon 2011;11:240–6.
48. Hosoya M, Shigeta S, Mori S, Tomoda A, Shiraishi S, Miike T, et al. High-dose intravenous ribavirin therapy for subacute sclerosing panencephalitis. Antimicrob Agents Chemother 2001;45:943–5.
49. Dunn LA, Fury MG, Sherman EJ, Ho AA, Katabi N, Haque SS, et al. Phase I study of induction chemotherapy with afatinib, ribavirin, and weekly carboplatin and paclitaxel for stage IVA/IVB human papillomavirus-associated oropharyngeal squamous cell cancer. Head Neck 2018;40:233–41.
50. Kosaka T, Maeda T, Shinojima T, Nagata H, Mizuno R, Oya M. A clinical study to evaluate the efficacy and safety of docetaxel with ribavirin in patients with progressive castration resistant prostate cancer who have previously received docetaxel alone. J Clin Oncol 2017;35:e14010.